Turkish Journal of Electrical Engineering & Computer Sciences

http://journals.tubitak.gov.tr/elektrik/

Research Article

Turk J Elec Eng & Comp Sci
(2019) 27: 973 – 984

doi:10.3906/elk-1708-20

Optimal range of loading for operating a fixed-speed wind turbine using a self-excited induction generator

Nassim IQTEIT[1], **Gül KURT**[2,*], **Bekir ÇAKIR**[2]

[1]Department of Electrical Engineering, Faculty of Engineering, Palestine Polytechnic University, Hebron, Palestine
[2]Department of Electrical Engineering, Faculty of Engineering, Kocaeli University, Kocaeli, Turkey

Received: 03.08.2017 • **Accepted/Published Online:** 10.12.2018 • **Final Version:** 22.03.2019

Abstract: In the present study, a new strategy of analysis was used to determine the optimal interval of a single-phase resistive load to operate a fixed-speed wind turbine. The essence of this optimal range is to enable the generator to have stable voltages and current balances, large power, and an acceptable frequency range, and also mitigate generator overheating. The generator windings and excitation capacitances were prepared according to the C-2C connection scheme with suitable values of excitation capacitances. The admittance matrix of the system was based on positive and negative sequence generator voltages and was calculated by symmetrical components theory. The generator performance was found through optimization of the determinant admittance matrix magnitude. Moreover, balanced position of the generator can be achieved near the maximum load power. Consequently, the best interval of resistive load of the generator (1.5 kW) was found around 2% voltage unbalance factor. The appropriate optimal load was approximately ±6% of the perfect balance resistive load value.

Key words: Fixed-speed wind turbine, C-2C connection, best interval of resistive loading, optimizing, balance position, self-excited induction generator

1. Introduction

Power supply in remote rural regions such as islands, military apparatus, ships, and villages is essential for the sustainable growth of a country. For most instances, wind energy is already available in these places and seems economical compared to other types of energy [1,2]. Since most of the resistive loads fed by isolated power systems are based on a single-phase system, a single-phase generator is a better choice. Generally, three-phase generator systems are widely used due to their advantages such as less maintenance, modest protection, and lower investment cost [3,4]. However, a three-phase induction machine can be modified to generation mode to supply single-phase load [5]. A three-phase squirrel cage induction machine is cheaper, it has good efficiency, and is available at higher power ratings (more than 3 kW) as well [3,6]. Furthermore, a squirrel cage machine can operate as a self-excited induction generator (SEIG). The excitation can be done using a capacitor bank connected to the stator windings of the induction generator. Magnetizing inductance is the most important factor in SEIG voltage build-up [7].

Wind turbine generating systems (WTGSs) can be classified under two main categories: fixed speed WTGSs and variable speed WTGSs. A variable speed WTGS contains advanced power electronic devices and control systems; therefore costs are high. On the other hand, the fixed speed of the WTGS has some

*Correspondence: gul.kurt@kocaeli.edu.tr

good advantages such as simple and lower probability of mechanical resonance, lack of harmonics, and lower investment cost [8].

The conversion of a three-phase SEIG to feed a single-phase load may result in unwanted performance. The drawbacks may include low generation efficiency, frequency variances, large voltage fluctuations, severe vibrations, and rising temperature. However, using suitable excitation capacitors, these unwanted effects can be alleviated by modified Steinmetz connection [9], Smith connection [6], or C-2C connection, which is a special case of the modified Steinmetz connection (i.e. $R_{auxiliary\,load} = \infty$ and Ca = 2Cm). Moreover, these connections of SEIGs and other types of connections were discussed in [10].

According to the literature, a number of studies have been published dealing with SEIG performance and models but only in three-phase loads [2,11,12]. In contrast, Chan and Lai proposed a method of phase balancing for a SEIG supplying single-phase resistive load, using the modified Steinmetz connection [9] and Smith connection [6]. Wang and Lee [13] also proposed a three-capacitor circuit scheme, as well as a method to estimate the values of self-excited capacitors, which allow the SEIG to be balanced. In another study, Anagreh and Iqteit [3] proposed a scheme that provides acceptable phase balance and large output power. Bhattacharya and Woodward [14] studied SEIG excitation balancing for maximum power output.

In research by Chan [15,16], balancing a SEIG with one excitation capacitor was investigated using single-phasing mode operation and Steinmetz connections I and II. The perfect balance operation was discovered when the induction generator runs reverse rotation. Alolah and Alkanhal [17] used a sequential genetic (GA)/gradient optimizer to minimize the unbalance between stator voltages. The authors noted that the maximum value of the unbalance factor does not exceed 7% at 0.5 load power factor (lagging) when the induction generator is excited by two shunt capacitors. Furthermore, the transient and steady-state model of a self-excited single-phase induction generator was proposed in [18] with an application of lighting an animal farm by biogas energy.

In the present study, the C-2C connection was used to simplify the analysis. To obtain the generator characteristics, a singular admittance matrix was derived by assigning positive and negative sequence generator voltages. Usually, remote rural areas have mostly resistive loads. When these loads are coupled with a SEIG at fixed speed wind turbine, the SEIG frequency and magnetizing reactance are changed. These values can be found through magnitude determinant optimization of the singular admittance matrix. The present research also presents the generator performances with different loads and different excitation capacitors. In addition, the main critical points of the generator, i.e. perfect balance point, maximum power point, and breakdown point, were determined.

This work presents an application to drive a SEIG by a fixed-speed wind turbine. Most of the literature focused only on the balancing condition of the SEIG when supplying single-phase load. However, the main contribution of this work is determining the best range of load demand to provide consumers with the best quality of frequency, voltage, and energy. In addition, the appropriate speed and excitation capacitors of the C-2C connection were specified to drive the SEIG at the best balancing conditions. The C-2C connection was used in this application due to its simplicity, costs, and perfect balance point. These optimal values and load range result in the reduction of initial operation cost, reduction in the unbalance effects of the SEIG, and supplying high-quality energy to consumers.

2. System connection and analysis model

Figure 1 shows the wind turbine system, including a fixed-speed wind turbine and induction generator. The C-2C connection is used as a delta connection and supplies a single-phase resistive load. Moreover, the generator is excited by the C-2C configuration method [6]. From the theories of wind energy, it is known that the wind turbine mechanical input power can be represented in terms of area swept by the rotor (A), air density (ρ), power coefficient (C_p), and wind speed (u) [12].

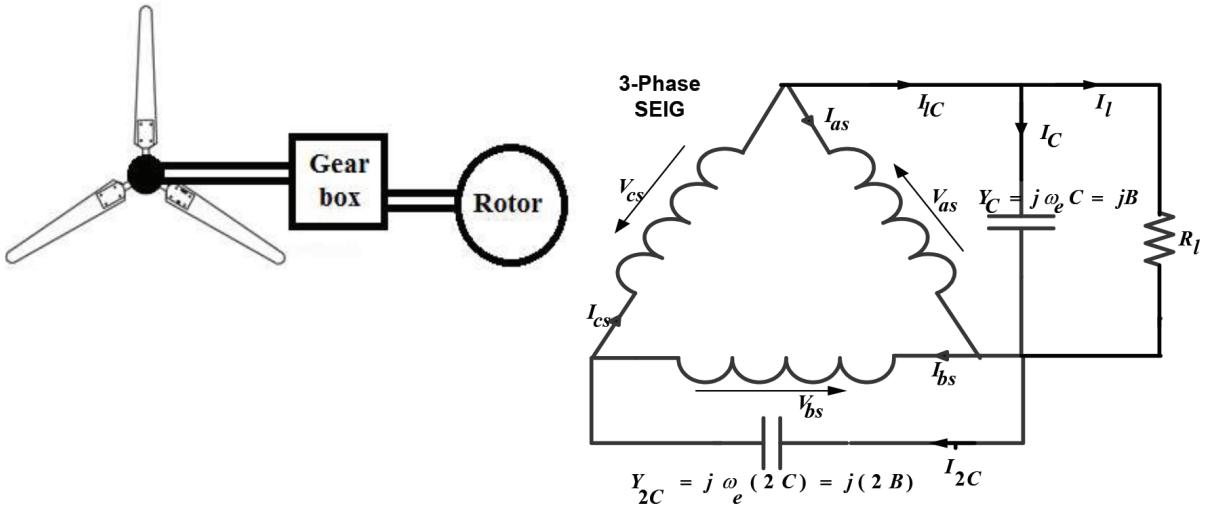

Figure 1. The C-2C connection of the SEIG with fixed speed wind turbine.

$$P_T = \frac{1}{2}\rho A u^3 C_p(\lambda), \tag{1}$$

where C_p depends on the tip speed ratio (λ), which can be calculated as

$$\lambda = \frac{\omega r}{u} \tag{2}$$

The relation between C_p and λ was obtained from the manufacturer of wind turbines. However, with modern turbines, a value $C_p \cong 0.5$ can be used, which is not far from the Betz limit ($C_{p\,max} = 16 \,/\, 27 \cong 0.59$) [8].

Depending on the circuit in Figure 1, the inspection equations (3) to (6) were obtained.

$$V_{as} + V_{bs} + V_{cs} = 0 \tag{3}$$

$$I_{lC} = I_C + I_l i_{lC} = i_C + i_l \tag{4}$$

$$I_l = \frac{V_{as}}{R_l} = G_l V_{as} \tag{5}$$

$$\begin{bmatrix} I_{as} \\ I_{bs} \\ I_{cs} \end{bmatrix} - \begin{bmatrix} I_{bs} \\ I_{cs} \\ I_{as} \end{bmatrix} = \begin{bmatrix} -(G_l + jB) & j(2B) & 0 \\ 0 & -j(2B) & 0 \\ (G_l + jB) & 0 & 0 \end{bmatrix} \begin{bmatrix} V_{as} \\ V_{bs} \\ V_{cs} \end{bmatrix} \tag{6}$$

By using symmetrical component theory and elimination of zero sequence of voltage and current [6], the stator phase voltages and currents can be expressed by

$$\begin{bmatrix} F_{as} \\ F_{bs} \\ F_{cs} \end{bmatrix} = \frac{1}{\sqrt{3}} \begin{bmatrix} 1 & 1 \\ a^2 & a \\ a & a^2 \end{bmatrix} \begin{bmatrix} F_{ps} \\ F_{ns} \end{bmatrix}, \tag{7}$$

where F is voltage V or current I.

When Eq. (6) is transformed into positive and negative sequence components, the result is expressed as follows in Eq. (8):

$$\begin{bmatrix} I_{ps} \\ I_{ns} \end{bmatrix} = \begin{bmatrix} -jB - \frac{1}{3}G_l & -\frac{1}{\sqrt{3}}B - \frac{1}{3}G_l \\ \frac{1}{\sqrt{3}}B - \frac{1}{3}G_l & -jB - \frac{1}{3}G_l \end{bmatrix} \begin{bmatrix} V_{ps} \\ V_{ns} \end{bmatrix} \tag{8}$$

Positive and negative sequence equivalent circuits of the SEIG, used for supplying a single-phase load at rated frequency, are given respectively in (a) and (b) of Figure 2 [19]. From Figure 2, the following equation can be obtained:

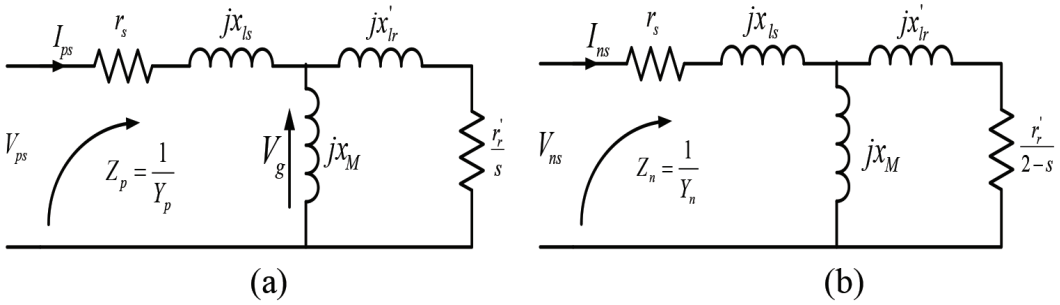

Figure 2. (a) Positive and (b) negative sequence equivalent circuits of the SEIG feeding a single-phase load at rated frequency.

$$\begin{bmatrix} I_{ps} \\ I_{ns} \end{bmatrix} = \begin{bmatrix} Y_p & 0 \\ 0 & Y_n \end{bmatrix} \begin{bmatrix} V_{ps} \\ V_{ns} \end{bmatrix} \tag{9}$$

Now subtracting Eq. (9) from (8) will result in Eq. (10).

$$\begin{bmatrix} 0 \\ 0 \end{bmatrix} = \begin{bmatrix} Y_p + jB + \frac{1}{3}G_l & \frac{1}{\sqrt{3}}B + \frac{1}{3}G_l \\ -\frac{1}{\sqrt{3}}B + \frac{1}{3}G_l & Y_n + jB + \frac{1}{3}G_l \end{bmatrix} \begin{bmatrix} V_{ps} \\ V_{ns} \end{bmatrix} \tag{10}$$

From Eq. (10) the expression of voltage unbalance factor (VUF) can be written as

$$VUF = \left|\frac{V_{ns}}{V_{ps}}\right| \times 100\% = \left|\frac{Y_p + \frac{2}{\sqrt{3}}B\angle 60^o}{Y_n + \frac{2}{\sqrt{3}}B\angle 120^o}\right| \times 100\%, \tag{11}$$

where Y_p and Y_n can be calculated from Figure 2.

From Eqs. (9) and (10), the expressions of current unbalance factor (CUF) can be written as

$$CUF = \left|\frac{I_{ns}}{I_{ps}}\right| \times 100\% = \left|\frac{Y_n V_{ns}}{Y_p V_{ps}}\right| \times 100\% = \left|\frac{Y_n}{Y_p}\right| VUF \tag{12}$$

Under steady-state self-excitation, $st \begin{bmatrix} V_{ps} \\ V_{ns} \end{bmatrix} \neq \begin{bmatrix} 0 \\ 0 \end{bmatrix}$; therefore, the coefficient matrix in Eq. (10) is a singular matrix, i.e.

$$f\left(X_M, F\right) = det\left(\begin{bmatrix} Y_p + jB + \frac{1}{3}G_l & \frac{1}{\sqrt{3}}B + \frac{1}{3}G_l \\ -\frac{1}{\sqrt{3}}B + \frac{1}{3}G_l & Y_n + jB + \frac{1}{3}G_l \end{bmatrix}\right) = 0 \tag{13}$$

For given values of excitation capacitances, load resistances, and speed, the values of F and X_M can be determined using Eq. (13), when the function $|f(X_M, F)|$ is minimum. In the present study, MATLAB code was used to solve the optimization problem to obtain the unknowns F and X_M. After determining F and X_M, the positive-sequence air gap voltage was found from the magnetization characteristic X_M – (Eg = Vg / F) (Appendix). Then the performance of the SEIG was computed and analyzed using Eqs. (3) to (12) and the circuits in Figure 2.

3. Perfect balance conditions

Modified Steinmetz and Smith connections can be used to achieve the perfect balance operation of a SEIG when single-phase resistive load is used. The perfect balance conditions of these connections are shown in Table 1, whereas the C-2C connection shown in Figure 1 is the perfect balance connection of the SEIG. This SEIG achieves the perfect balance point when the negative sequence voltage vanishes ($V_{ns} = 0$). According to Eq. (10) the perfect balance condition of C-2C is given by

$$\begin{cases} C = \frac{\sqrt{3}}{4\pi f}\left|Y_p\right| \\ \varphi_p = 120^o \end{cases} \tag{14}$$

Table 1. Perfect balance connections of SEIG.

	Modified Steinmetz [9]	Smith [6]	C-2C
Perfect balance conditions at purely resistive load	$C_2 = 2C_3 = \frac{\sqrt{3}}{2\pi f}\left\|Y_p\right\|$ $\varphi_p = 120^o$ At removed auxiliary load (R_{L2})	$C_1 = \frac{C_2}{2} = C_3 = \frac{1}{2\sqrt{7}\pi f}\left\|Y_p\right\|$ $\varphi_p = tan^{-1}\left(\frac{-2}{\sqrt{3}}\right) = 130.9^o$	$C = \frac{\sqrt{3}}{4\pi f}\left\|Y_p\right\|$ $\varphi_p = 120^o$

4. The strategy of system analysis

Usually, electric systems in remote rural areas are not complex and must have low initial costs. For these reasons, a fixed-speed wind turbine, SEIG, and single-phase network are usually preferable. System protection and maintenance cost reduction, together with generator components, sustainability, and consumers' satisfaction in using frequency and voltage service, are the main targets of this research.

The negative effects of unbalanced voltage on three-phase induction machines are rising machine temperature, increasing losses, decreasing machine efficiency, and reduction in generated power [20]. Wind turbines must run in normal conditions (90%–105% voltage and 49–51 Hz), but should also be able to work outside of these ranges within identified time limits [21].

Unbalanced currents in stator windings occur due to the nonequal line voltage of the SEIG. The deviation in frequency should not exceed ±5% if the voltage is at the rated value, while the variation in voltage should not exceed ±10% if the frequency is at the rated value [22]. Through these limitations and association with

perfect balance point, maximum power point, and breakdown point, the best loading interval of the SEIG can be found.

According to the National Electrical Manufacturers Association, the percentage of unbalanced voltage is given by

$$V_{unbalance} = \frac{\max.\ unbalance\,voltage\ -\ rated\,voltage}{rated\,voltage} \times 100\% \tag{15}$$

Consequently, the flowchart shown in Figure 3 explains the selection procedure of the optimal loading range of the SEIG under unbalanced loading current.

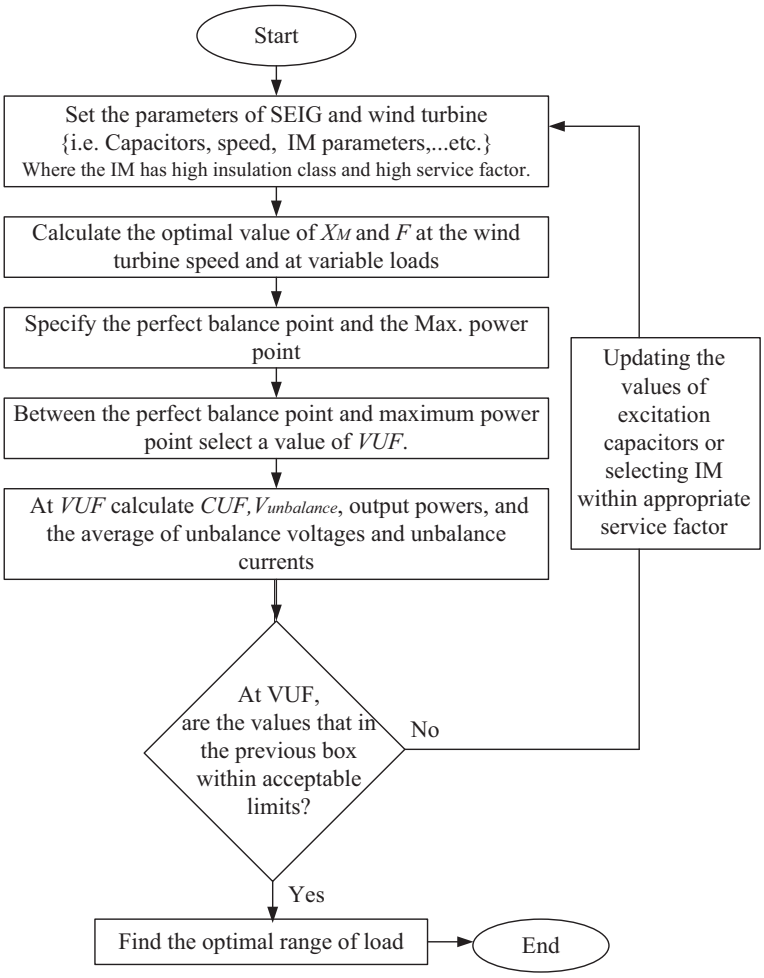

Figure 3. Flowchart for selecting the procedure of the optimal loading range of the SEIG.

5. Results and discussion

The squirrel cage machine was simulated when a fixed speed wind turbine was connected as a prime mover. The wind turbine provided a constant speed that is greater than synchronous speed. Induction generator parameters and magnetization characteristic and base values are given in the Appendix [3].

5.1. Performance of the SEIG and critical operation points

Figures 4 to 6 show the performance and critical points operation of the SEIG when driven by a wind turbine at fixed speed 1515 rpm and excited with capacitors at 40 μF. Figure 4 shows the change in load power, load voltage, and *VUF* with load current. The critical points, perfect balance point, maximum power point, and breakdown point are also presented in the same figure (Figure 4). Additionally, this figure shows that the voltage unbalance factor at the load that gives the maximum power is equal to 5.822%, while the SEIG reaches breakdown when *VUF* is greater than 7.845%. Figure 5 shows the variation in the magnitude and angle of *VUF* with load current. At load current 1.11 pu the *VUF* equals zero, its angle jump is 48.77°, and the generator reaches the balance position. Figure 6 shows the variation in the frequency and *VUF* with load resistance. The balancing resistance is 0.79 pu and the frequency of the generator equals 0.9803 pu. Moreover, the frequency at the maximum power is 0.9689 pu and resistance maximum power equals 0.49 pu. Furthermore, Figure 6 illustrates that the frequency and *VUF* linearly increase when the load resistance is greater than 2 pu.

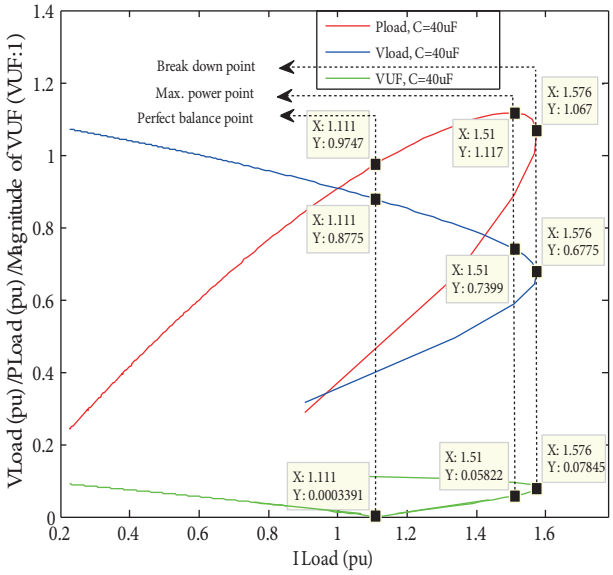

Figure 4. Variation in the load power, load voltage, and magnitude of *VUF* with load current.

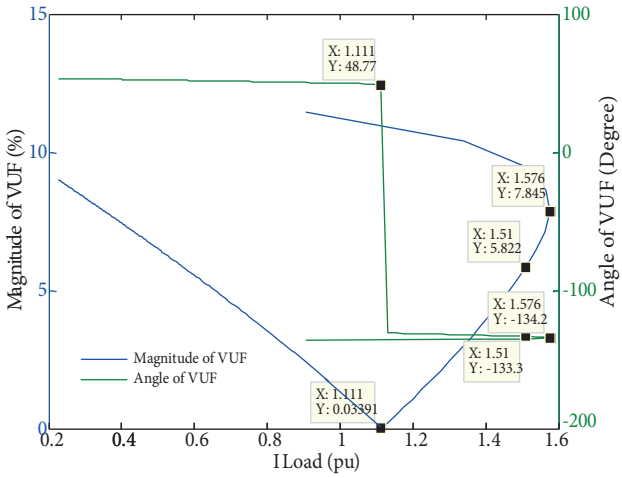

Figure 5. Variation in the magnitude and angle of *VUF* with load current.

5.2. SEIG characteristics with different excited capacitors

Figures 7 to 10 show the generator characteristics when driven at fixed speed 1515 rpm, with excitation capacitors values of 37 μF, 40 μF, and 43 μF. Figure 7 shows the resistive loads characteristics of $RL1_b$, $RL2_b$, and $RL3_b$ at perfect balance points and the characteristics of $RL1_m$, $RL2_m$, and $RL3_m$ at maximum power points of the generator, respectively. At the excitation capacitors mentioned above, the ranges of resistive loads between maximum power point and balance point ($\{RL_m$, $RL_b\}$) are {0.63, 0.93},{0.49, 0.79}, and {0.47, 0.73}, respectively. Figure 8 shows the variation in the frequency with load power for different capacitors excitation. The variation frequency curve dramatically dropped between the balance power point and the maximum power point. This effect can be seen when the characteristic generates at 40 μF. In addition, Figures 7 and 8 show that the load voltage and the frequency can be easily controlled by changing the value of the excitation capacitors. Figure 9 shows the relation between total reactive power and load voltage. From this figure, the following

conclusions were observed: at balance voltage, the total reactive power equals zero; it is negative between balance voltages and maximum power and positive when the load voltage is greater than balance voltage. In addition, between the perfect balance and maximum power positions, the generator has a linear characteristic ($Q_{total} - V_{load}$ curves having approximately the same slope). Figure 10 shows the relation between real load power and total reactive power. It also shows that the curve of $P_{Load} - Q_{total}$ decreases between balance and maximum power position. Additionally, it should be noted that the area inside the capability curves shown in Figure 10 increases when the values of the excitation capacitors are increased. Table 2 summarizes the characteristics of the system shown in Figure 1 at different types of operation points when the excited capacitor C = 40 μF and the speed of the wind turbine is equal to 1515 rpm. For example, the voltage unbalance factor was equal to zero at the perfect balance point. At this point, the total reactive power was also equal to zero and the current and the voltage of the windings reached a state of balance. However, when comparing the results from Figures 4 to 10 together with the acceptable limitations, it can be concluded as, at 1515 rpm speed and 40 μF excitation capacitor value, the load is not suitable for the supply because it is outside the acceptable ranges.

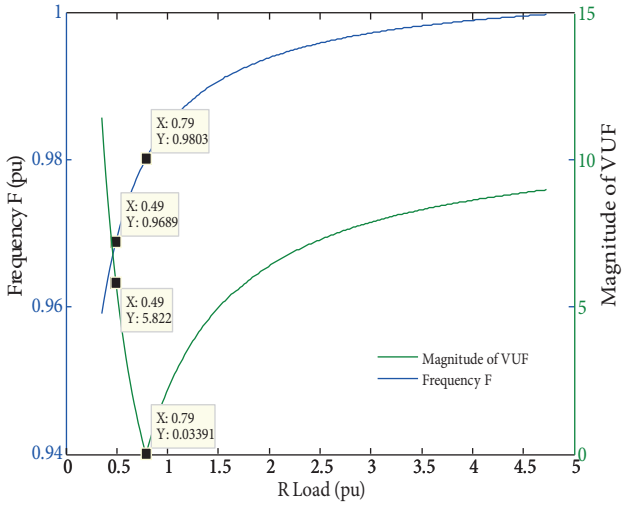

Figure 6. Variation in the frequency and magnitude of *VUF* with load resistance.

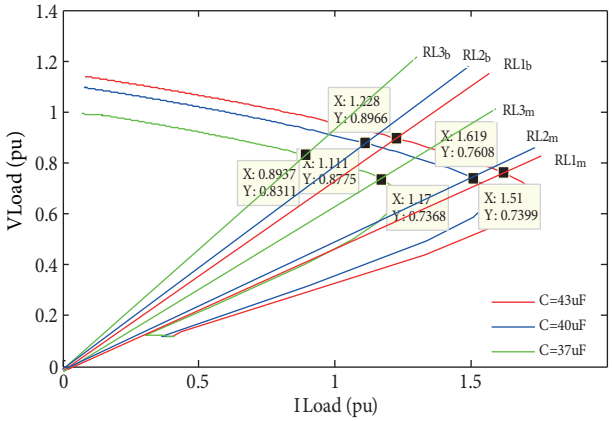

Figure 7. Loading resistors at perfect balance points and maximum power point for different C values.

Table 2. The best important operation points of the SEIG at excited capacitor C = 40 μF and wind turbine speed 1515 rpm.

VUF	F	I $_{load}$	I_{as}	I_{bs}	I_{cs}	V_{load} =V_{as}	V_{bs}	V_{cs}	P_{Load}	Q_{total}	Type of
(%)	(pu)	(pu)	(pu)	(pu)		(pu)	(pu)	(pu)	(pu)	(pu)	point
7.845	0.9653	1.576	0.8657	0.4305	0.839	0.6775	0.7023	0.77	1.067	–0.01931	B.D.P
5.822	0.9689	1.51	0.8425	0.5072	0.8379	0.7399	0.7582	0.8136	1.117	–0.01530	M.P.P
2.09	0.976	1.275	0.7705	0.6522	0.7841	0.8286	0.8348	0.8574	1.056	–0.00537	Min.R.P
≅ 0.0	0.9803	1.111	0.744	0.744	0.744	0.8775	0.8775	0.8775	0.9747	≅ 0.0000	P.B.P
2.095	0.9846	0.9337	0.7336	0.8389	0.6939	0.9243	0.9188	0.8932	0.863	+0.004584	Max.R.P

B.D.P: Breakdown Point, M.P.P: Max. Power Point, Min.R.P: Min. Range Point, Max. Range Point, P.B.P: Perfect Balance Point.

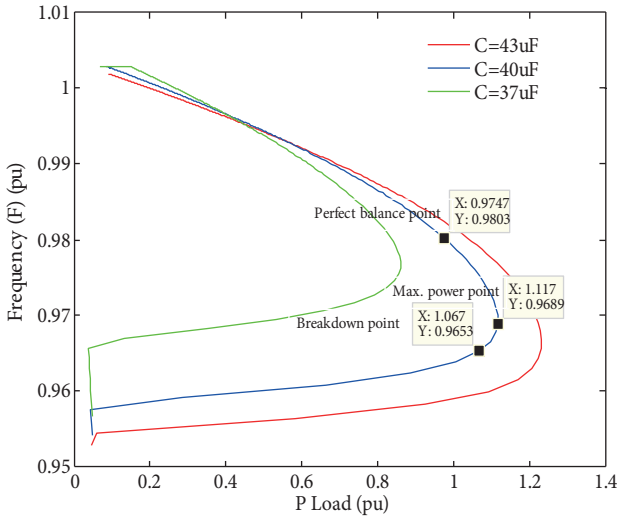

Figure 8. Frequency with load power for different values of C.

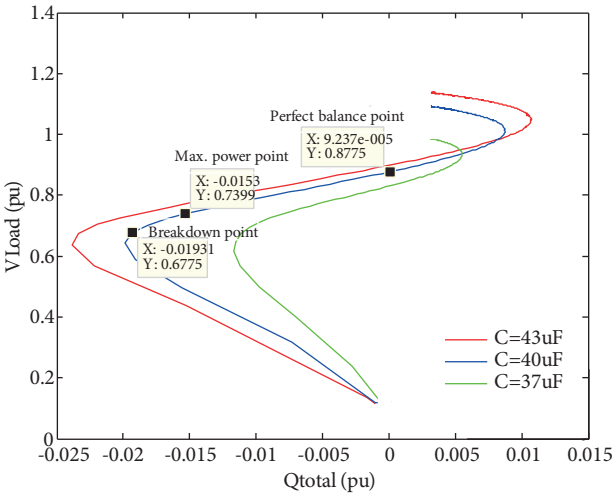

Figure 9. Variation in the load voltage with total reactive power for different C values.

5.3. Selecting the optimal interval loading

The following parameters are important for selecting the best load interval: *VUF*, *CUF*, load power, load voltage, load current, total reactive power, and frequency of the system. Taking into account the previous acceptable limitations, compilation of the parameters' variation according to *VUF* helps in determining the best interval load as shown in Figure 11. After exciting the generator with C = 60 μF capacitors and 1530 rpm speed, the perfect balance line and maximum power line helped to determine the best interval load. Figure 11 and Table 3 show that when the deviation of the frequency –3% $\in$ [–5, 5]%, the average of voltage is equal to 0.9987 at *VUF* = 1.88%. Therefore, this condition agrees with the strategy of selecting the optimal interval load. However, at the maximum limit of load interval, the average value of unbalance currents was equal to 1.285 pu. There is a large probability that this overcurrent causes overheating in the winding of the SEIG, but this problem can be solved by selecting an appropriate insulation class and a high service factor of induction machine [23] or by reducing the excitation capacitor to less than 60 μF but this solution will change the service voltage. However, Table 3 reports the parameter variation values suitable for the determination of the best interval loads. The best load interval was determined as [0.47, 0.6023] pu. All parameters determined in this study almost matched the limitation values according to the analysis strategy.

Table 3. Generator and load parameters at ends of optimal interval loading.

Interval	*VUF* (%)	*CUF* (%)	F (pu)	I $_{load}$ (pu)	V$_{load}$ (pu)	P$_{Load}$ (pu)	Q$_{Total}$ (pu)	R$_{Load}$(pu)
Maximum	1.88	7.106	0.9754	1.73	1.042	1.803	0.007784	0.6023 (max.)
Minimum	1.88	6.972	0.9693	2.033	0.9555	1.943	–0.008084	0.47 (min.)
Interval	V$_{as}$ (pu)	V$_{bs}$ (pu)	V$_{cs}$ (pu)	$V_{unbalance}$(%)	I$_{as}$ (pu)	I$_{bs}$ (pu)	I$_{cs}$ (pu)	$I_{unbalance}$(%)
Maximum	1.042	1.034	1.01	1.296	1.266	1.371	1.218 (min)	6.693
Minimum	0.9555	0.9646	0.9861	1.793	1.262	1.151	1.294 (max)	4.721

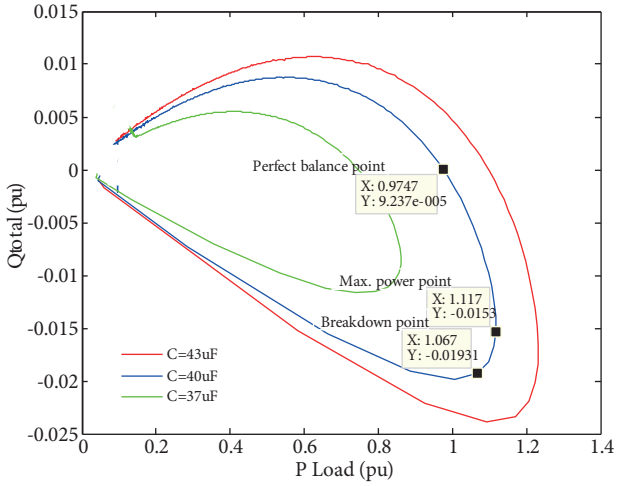

Figure 10. Variation in the load power with total reactive power for different values of C.

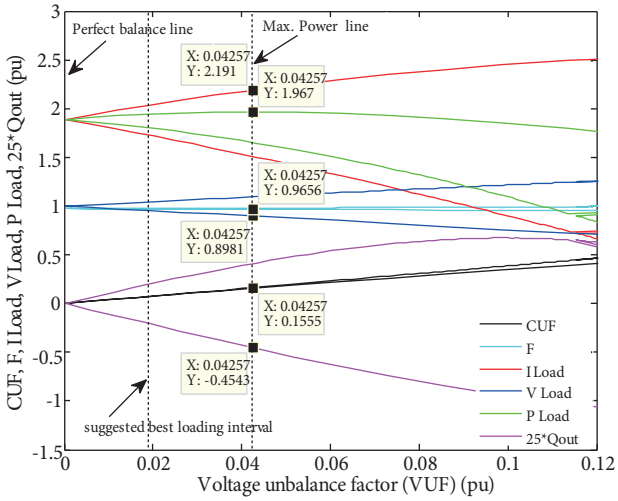

Figure 11. Determination of the best interval loading of the SEIG through different variables.

6. Conclusions

Green energy has become a very important area in energy generation due to the problems associated with fossil fuels. This research revealed that by using the C-2C connection with suitable values of excitation capacitance the interval between the balanced position and the maximum load power of a generator is considerably diminished (about 4% of *VUF*). The best interval load of the generator was found around 2% *VUF*. Approximately, ±6% of the perfect balance resistive load value was determined as the best optimal level. Application of the values obtained in this study in a three-phase generator would generate more energy and mitigate overheating of the system. Most importantly, from an economic point of view, it is a very simple system to set up.

List of symbols

a	Complex operator $e^{j\frac{2\pi}{3}}$
A	Area swept by the rotor of wind turbine
B	Susceptance
C	Capacitance
C_p	Power coefficient of wind turbine
E_g	Internal generated voltage
F	Per unit frequency f/f_{base}
f	Frequency
G_l	Conductance load $= 1/R_l$
I_C, I_{2C}	Current through capacitances
I_l	Load current
I_{as}, I_{bs}, I_{cs}	a, b, c phase stator currents
I_{ps}, I_{ns}	Positive and negative sequence stator currents
j	Imaginary number $\sqrt{-1}$
P_T	Wind turbine generator mechanical input power
P_{out}	Output power
Q_{out}	Total reactive power in the system
R_l	Resistive load
r	Turbine rotor radius
r_s, $r\acute{}_r$	Resistances of stator and rotor (referred to stator)

s	Slip
u	Wind speed
V_{as}, V_{bs}, V_{cs}	a, b, c phases stator voltages
x_{ls}, x'_{lr}	Leakage inductances of stator and rotor (referred to stator)
x_M	Magnetizing reactance
$Y_p Y_n$	Positive and negative admittance of induction generator
$Z_p Z_n$	Positive and negative impedance of induction generator
VUF	The ratio of negative–positive sequence voltages
CUF	The ratio of negative–positive sequence currents
λ	Wind turbine tip speed ratio
ω	Angular velocity of rotor wind turbine
ω_b	Base speed
ω_e	Synchronous generator speed

References

[1] Mahato S, Sharma M, Singh S. Transient performance of a single-phase self-regulated self-excited induction generator using a three-phase machine. Electr Pow Syst Res 2007; 77: 839-850.

[2] Benlamoudi A, Abdessemed R. Autonomous SEIG in a small wind power plant with voltage and frequency control. Serbian Journal of Electrical Engineering 2012; 9: 343-359.

[3] Anagreh Y, Iqteit N, Mohammad S. Performance analysis of a new configuration of three-phase self-excited induction generator feeding a single-phase load. International Journal of Power and Energy Conversion 2013; 4: 167-181.

[4] Omer A. Environmental and socio-economic aspects of possible development in renewable energy use. Journal of Agricultural Extension and Rural Development 2010; 2: 1-21.

[5] Singh B, Saxena R, Murthy S, Singh BP. A single-phase self-excited induction generator for lighting loads in remote areas. Int J Elec Eng Educ 1988; 25: 269-275.

[6] Chan T, Lai L. A novel excitation scheme for a stand-alone three-phase induction generator supplying single-phase loads. IEEE T Energy Conver 2004; 19: 136-143.

[7] Seyoum D, Grantham C, Rahman M. The dynamic characteristics of an isolated self-excited induction generator driven by a wind turbine. IEEE T Ind Appl 2003; 39: 936-944.

[8] ABB. Technical Application Papers. Wind power plants, Bergamo, Italy, 2011.

[9] Chan T, Loi L. Steady-state analysis and performance of a stand-alone three-phase induction generator with asymmetrically connected load impedances and excitation capacitances. IEEE T Energy Conver 2001; 16: 327-333.

[10] Ion CP, Marinescu C. Three-phase induction generators for single-phase power generation: an overview. Renewable and Sustainable Energy Reviews 2013; 22: 73-80.

[11] Neam MM, El-Sousy FFM, Ghazy MA, Abo-Adma MA. The dynamic performance of an isolated self-excited induction generator driven by a variable-speed wind turbine. 2007 International Conference on Clean Electrical Power; 21–23 May 2007; Capri, Itlay: IEEE. pp. 536-543.

[12] Balci ME, Hocaoglu MH, Koksoy A, Ozturk O, Dursun B. A fixed speed induction generator model for unbalanced power flow analysis. 2014 16th International Conference on Harmonics and Quality of Power (ICHQP); 25–28 May 2014; Bucharest, Romania: IEEE. pp. 209-213.

[13] Wang Y, Lee M. A method for balancing a single-phase loaded three-phase induction generator. Energies 2012; 5: 3534-3549.

[14] Bhattacharya J, Woodward J. Excitation balancing of a self-excited induction generator for maximum power output. IEE Proceedings C Generation, Transmission and Distribution; March 1988; 135: IET. pp. 88-97.

[15] Chan T. Performance analysis of a three-phase induction generator connected to a single-phase power system. IEEE T Energy Conver 1998; 13: 205-213.

[16] Chan T. Performance analysis of a three-phase induction generator self-excited with a single capacitance. IEEE Power Engineering Society 1998 Winter Meeting; 1–5 February 1998; Tampa, FL, USA: Paper No. PE- 028-EC-0-10-1997.

[17] Alolah AI, Alkanhal MA. Excitation requirements of three-phase self-excited induction generator under single-phase loading with minimum unbalance. Proceedings of IEEE Power Engineering Society Winter Meeting; 23–27 January 2000, Singapore, Singapore; IEEE. pp. 257-259.

[18] Iqteit NA, Daud AK. A new model of self-excited induction generator to feed a single phase load with an application in lighting animal farm. International Journal of Power and Energy Conversion 2019; 10: 32-50. DOI: 10.1504/IJPEC.2019.096721.

[19] Chapman S. Electric Machinery Fundamentals. New York, NY, USA: McGraw-Hill, 1985.

[20] Williams JE. Operation of 3-phase induction motors on unbalanced voltages [includes discussion]. Transactions of the American Institute of Electrical Engineers Part III: Power Apparatus and Systems. 1954; 73: IEEE. pp. 125-133.

[21] Chen Z. Issues of connecting wind farms into power systems. IEEE/PES Transmission & Distribution Conference & Exposition: Asia and Pacific; 18–18 Aug. 2005; Dalian, China: IEEE. pp. 1-6.

[22] Engineering Data, Integral AC motor selection and application guide for fans, Technical report, Twin City Fan Companies, November 1999.

[23] EEP. Guide to specification of electric motors. Electrical Engineering Portal, 2018.

Appendix

- Induction generator

1.5 kW, 3 phase, 4 pole, 50 Hz, line to line voltage (V) 220Δ/380Y, line to line current (A) 6.4 Δ/3.7 Y, 1415 rpm, 0.77 lagging power factor,

$r_s = 5.027\ \Omega,\ r'_r = 3.51\ \Omega, X_{ls} = 5.78\ \Omega,\ X'_{lr} = 5.78\ \Omega,\ X_M = 98.92\ \Omega.$ The relationship between $E_g = \frac{V_g}{F}$ *and* X_M is given by

$$E_g = -0.1314\,X_M^5 + 0.7269\,X_M^4 - 1.4118\,X_M^3 + 1.1262\,X_M^2 - 0.6172\,X_M + 1.4779$$

- Base values

base voltage (V_{base}) = 220 V, base current (I_{base}) = 3.7 A,

base power (P_{base}) = 220 $\times$3.7 = 814 W, base impedance (Z_{base}) = 59.5 Ω.